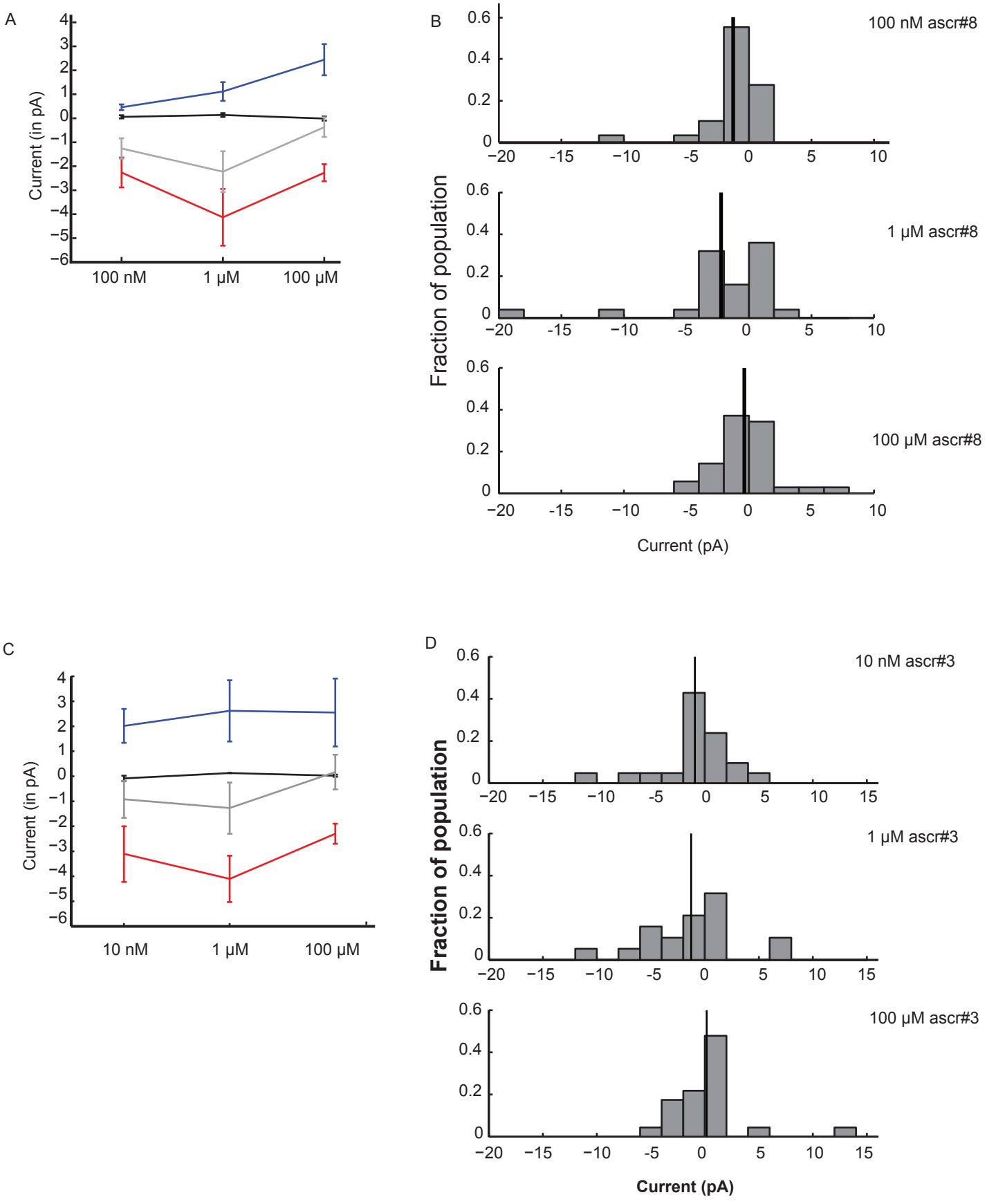

Supplementary Figure S1

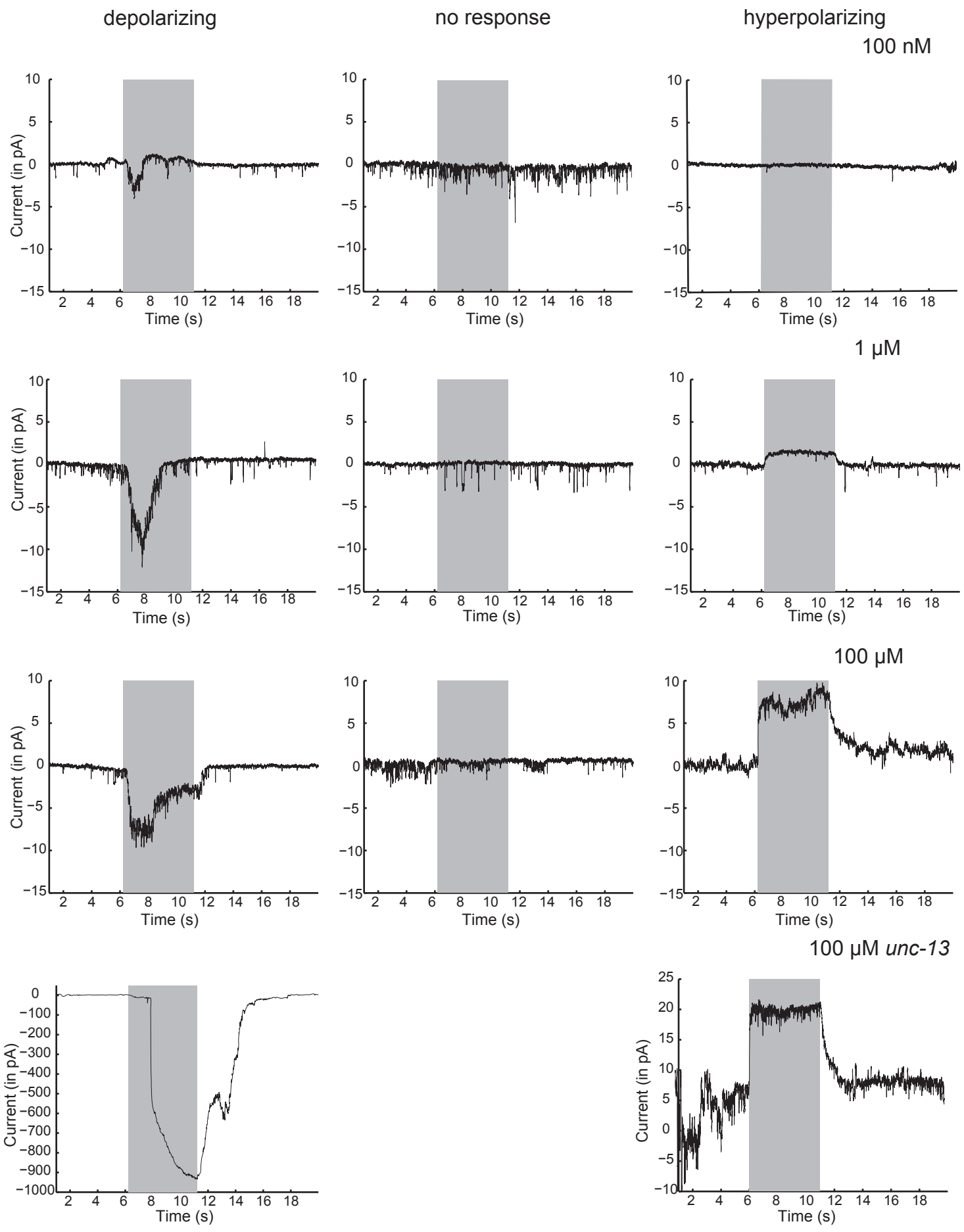

Supplementary Figure S2

A

ascr#8

Cells pooled across concentrations

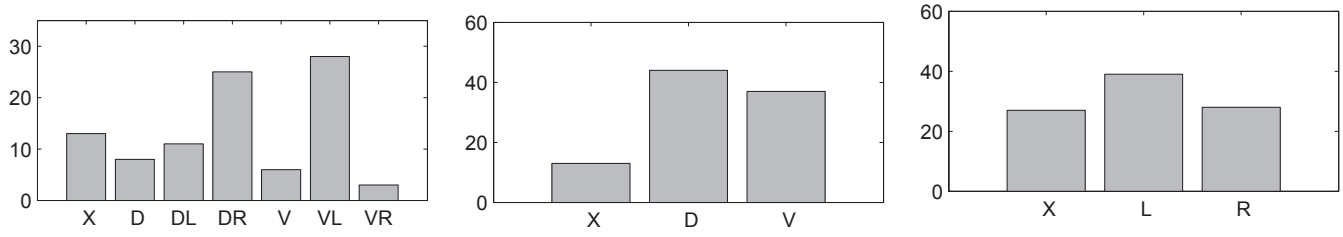

B

Pooled across concentrations, classified by response mode

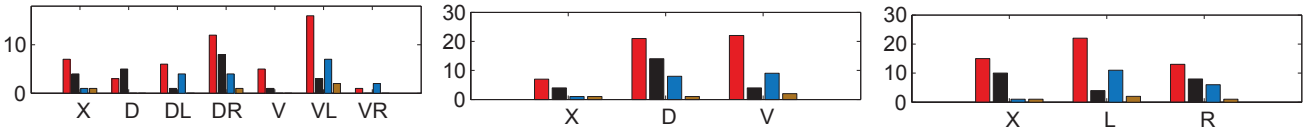

100 nM

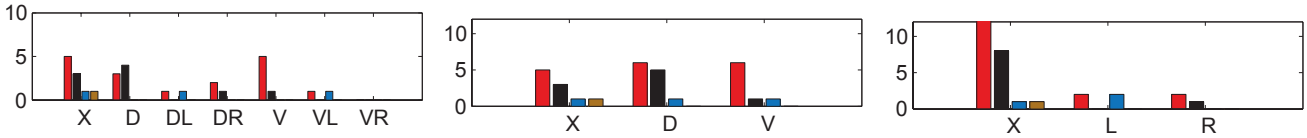

1 µM

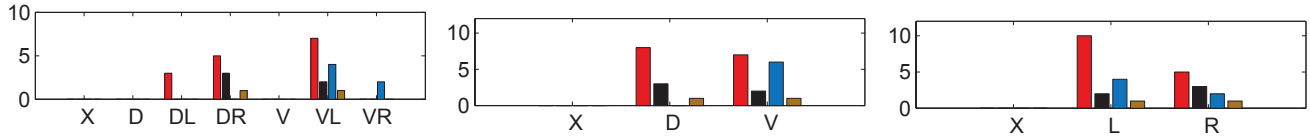

100 µM

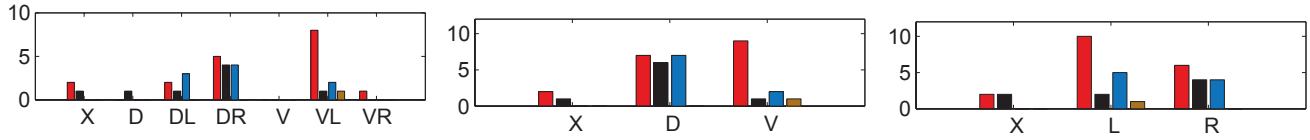

100 µM, *unc-13*

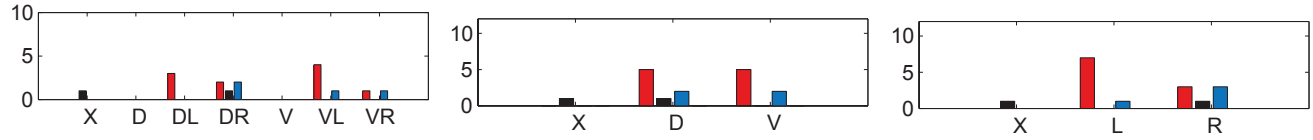

Supplementary Figure S3

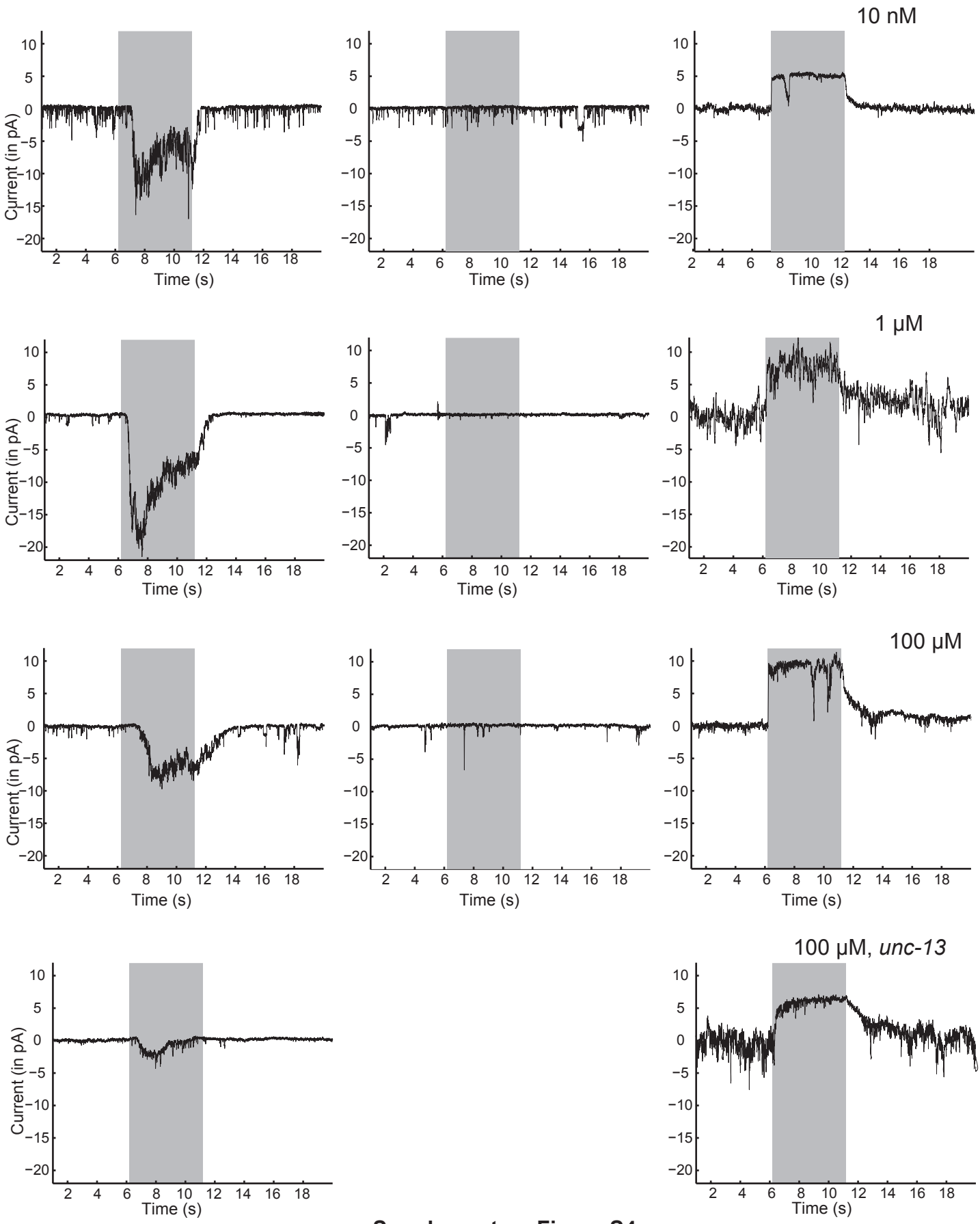

Supplementary Figure S4

A

ascr#3

Cells pooled across concentrations

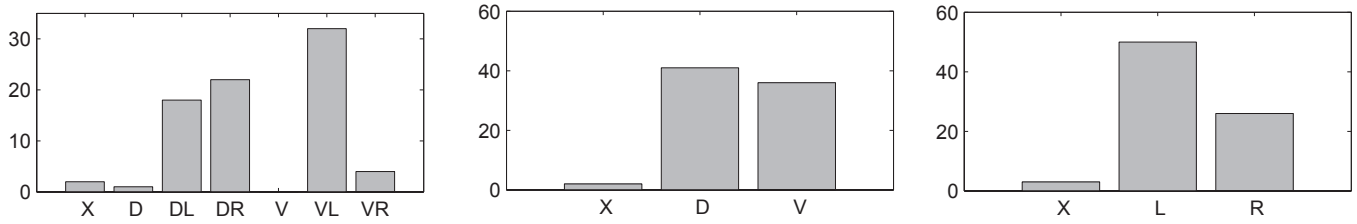

B

Pooled across concentrations, classified by response mode

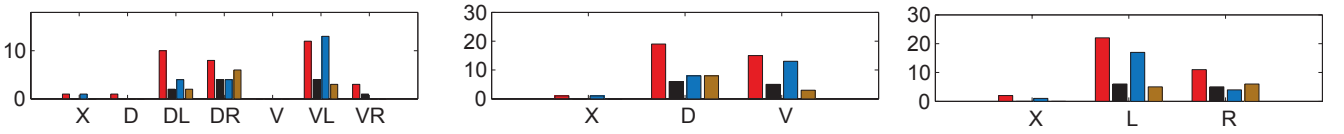

10 nM

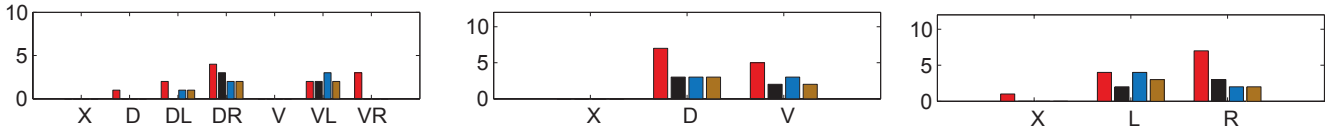

1 µM

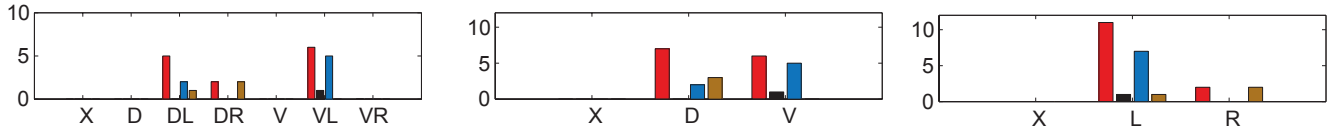

100 µM

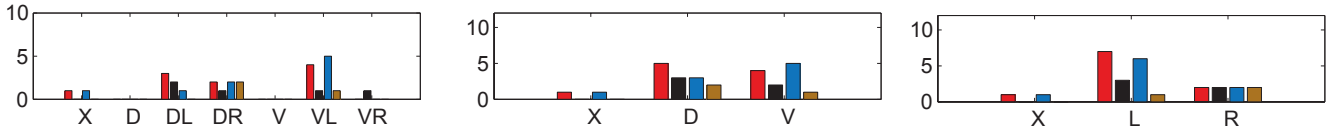

100 µM, *unc-13*

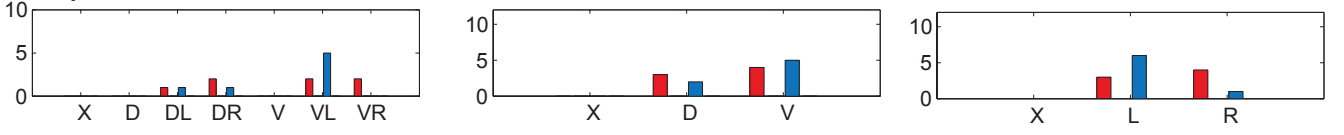

Supplementary Figure S5

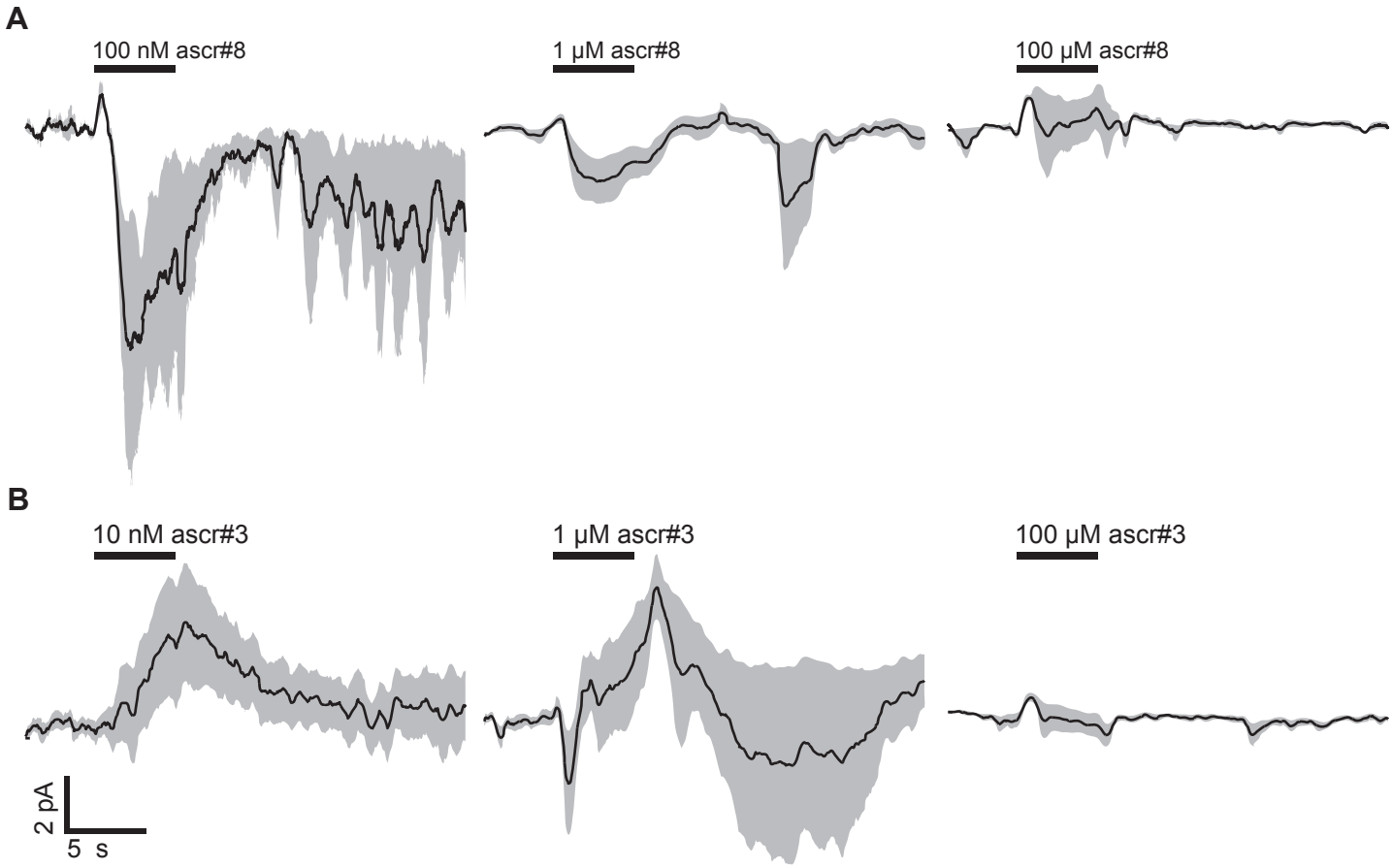

Supplementary Figure S6

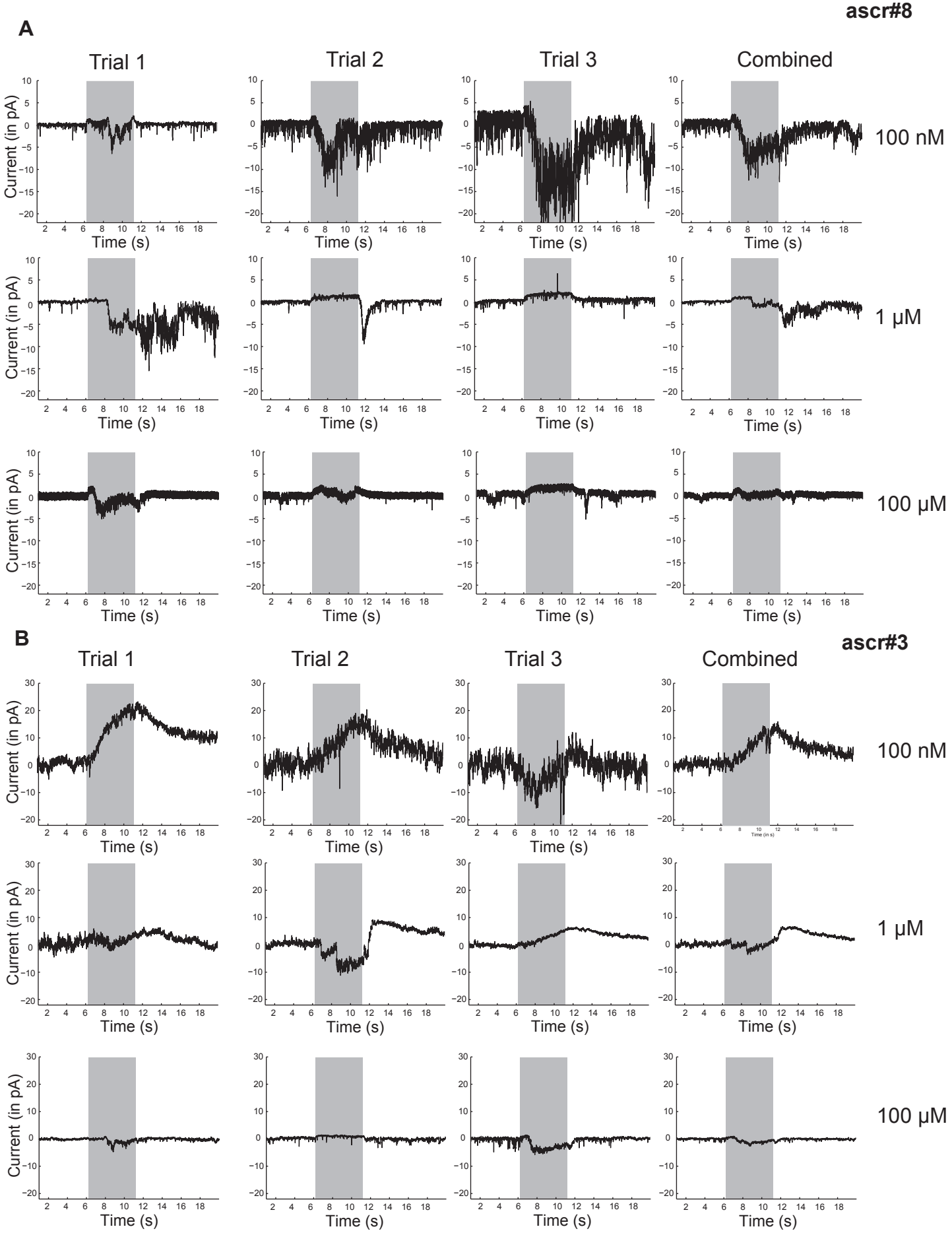

Supplementary Figure S7

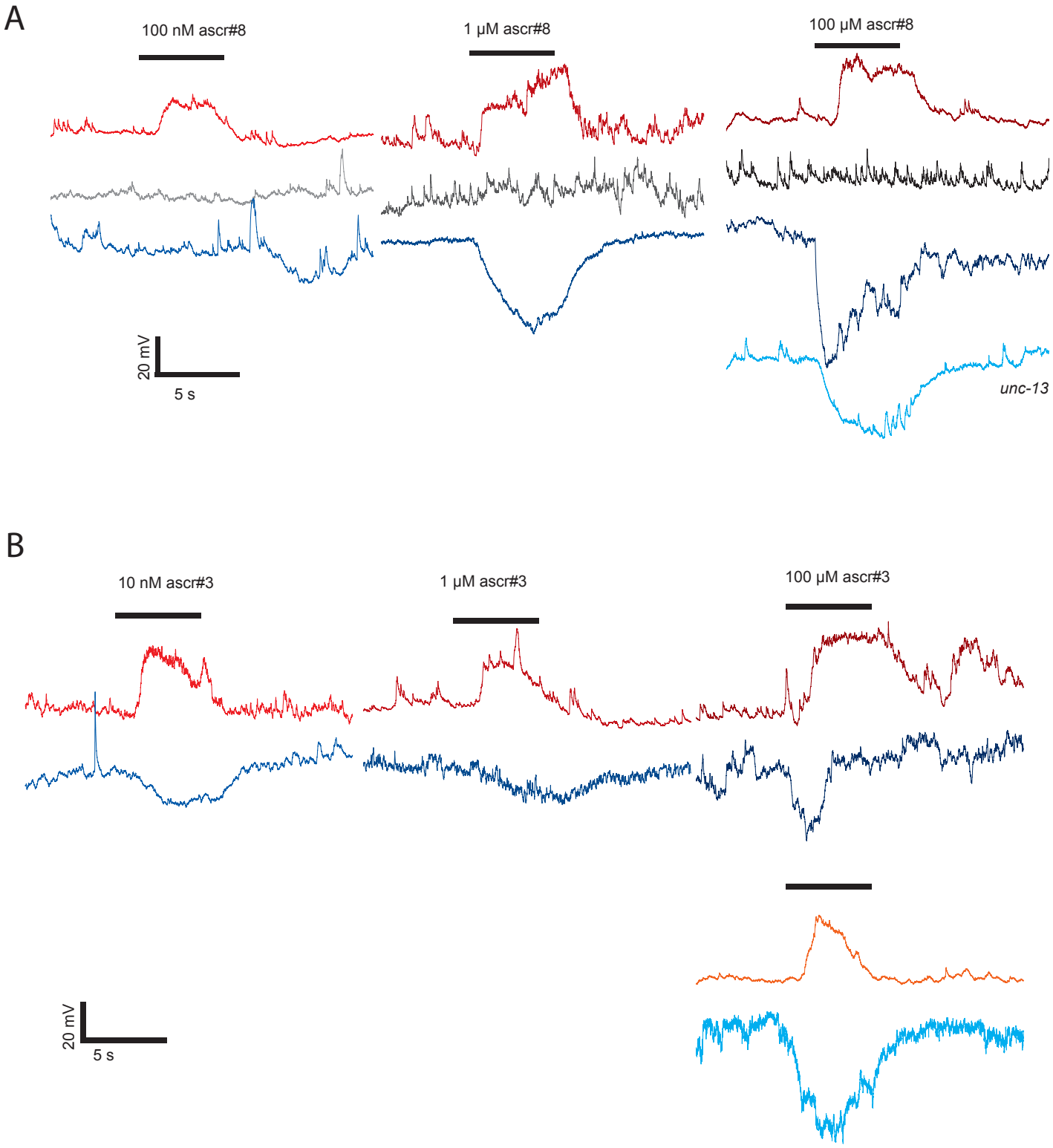

Supplementary Figure S8

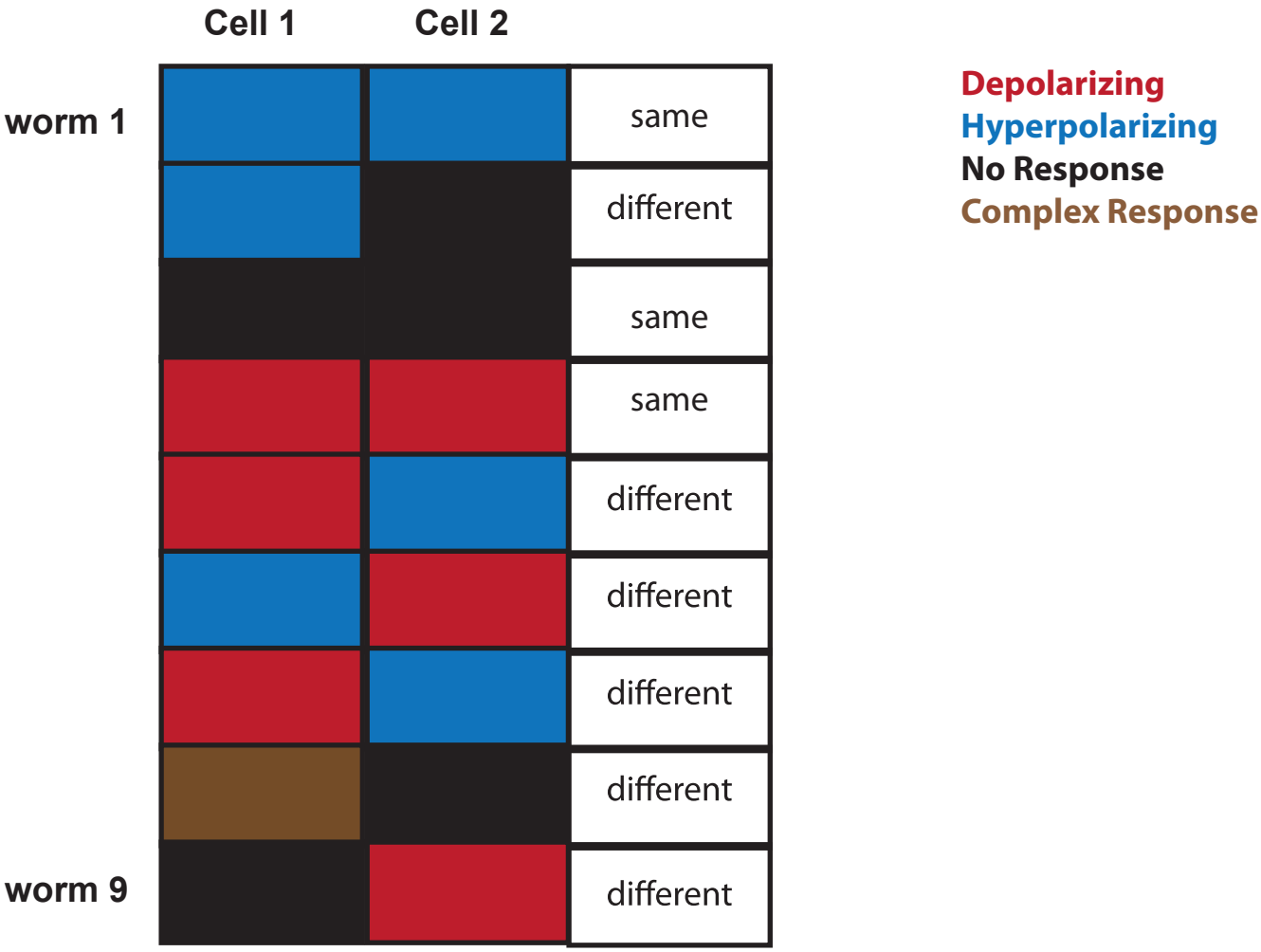

Supplementary Figure S9

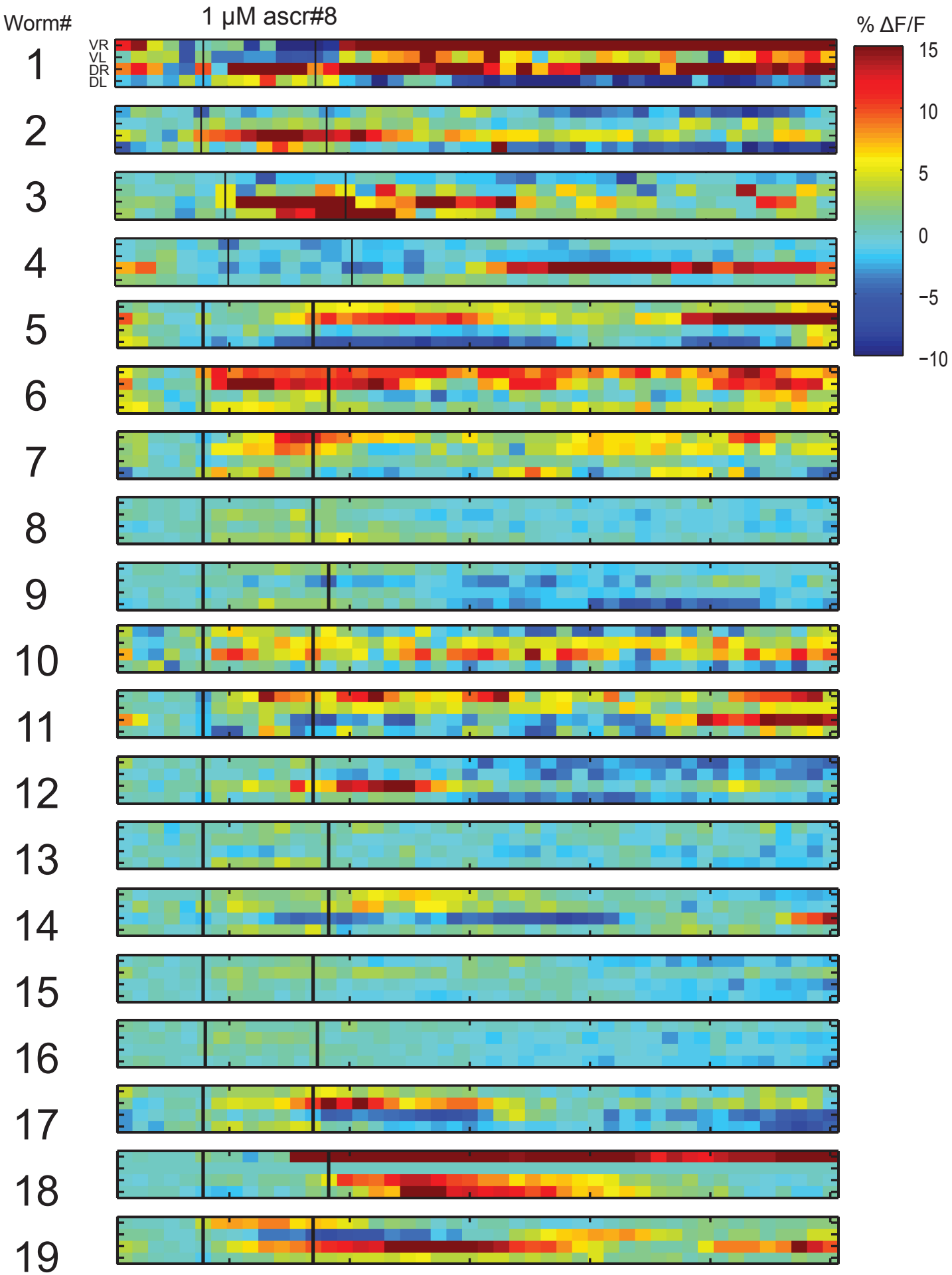

Supplementary Figure S10

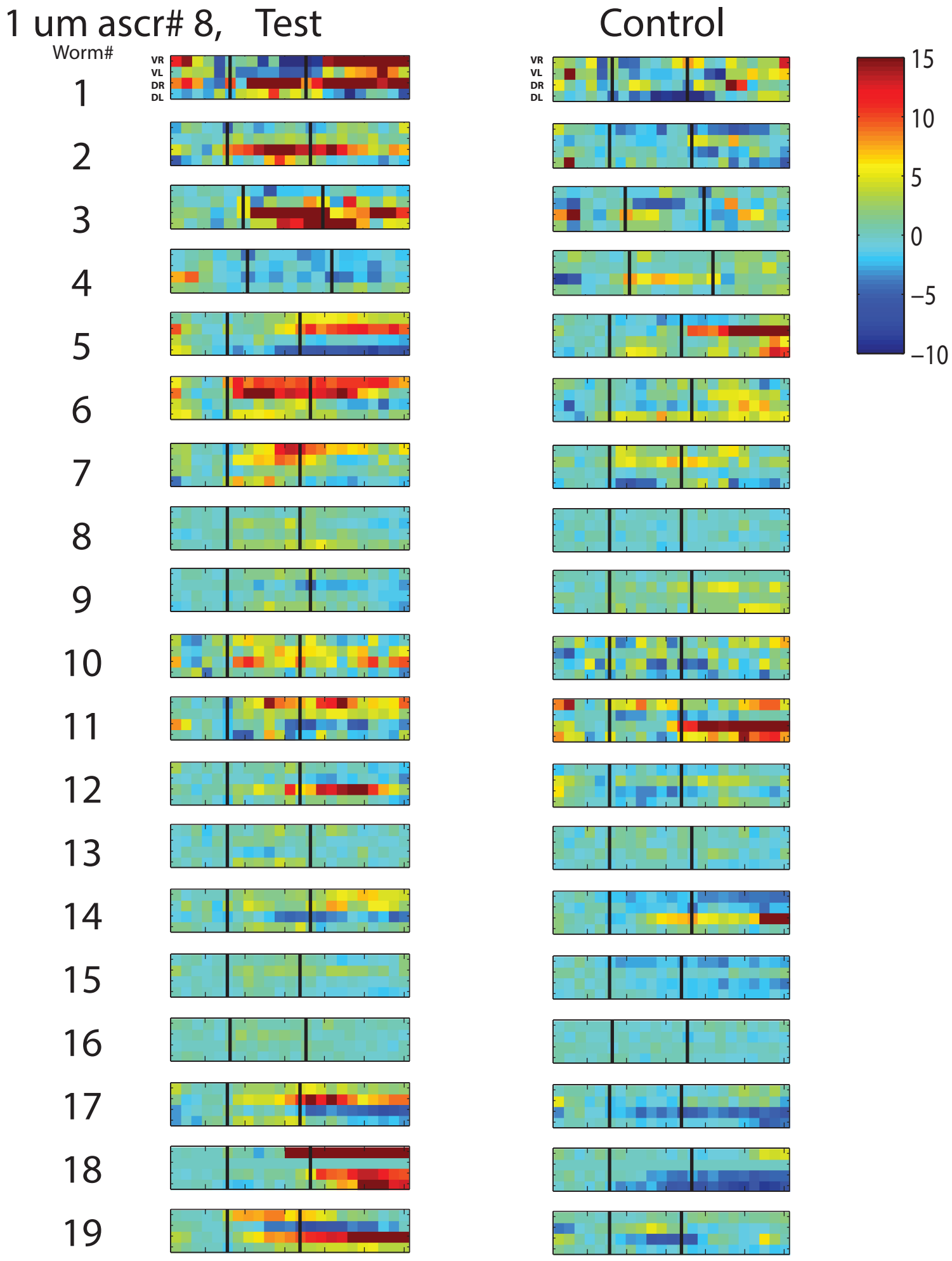

Supplementary Figure S11

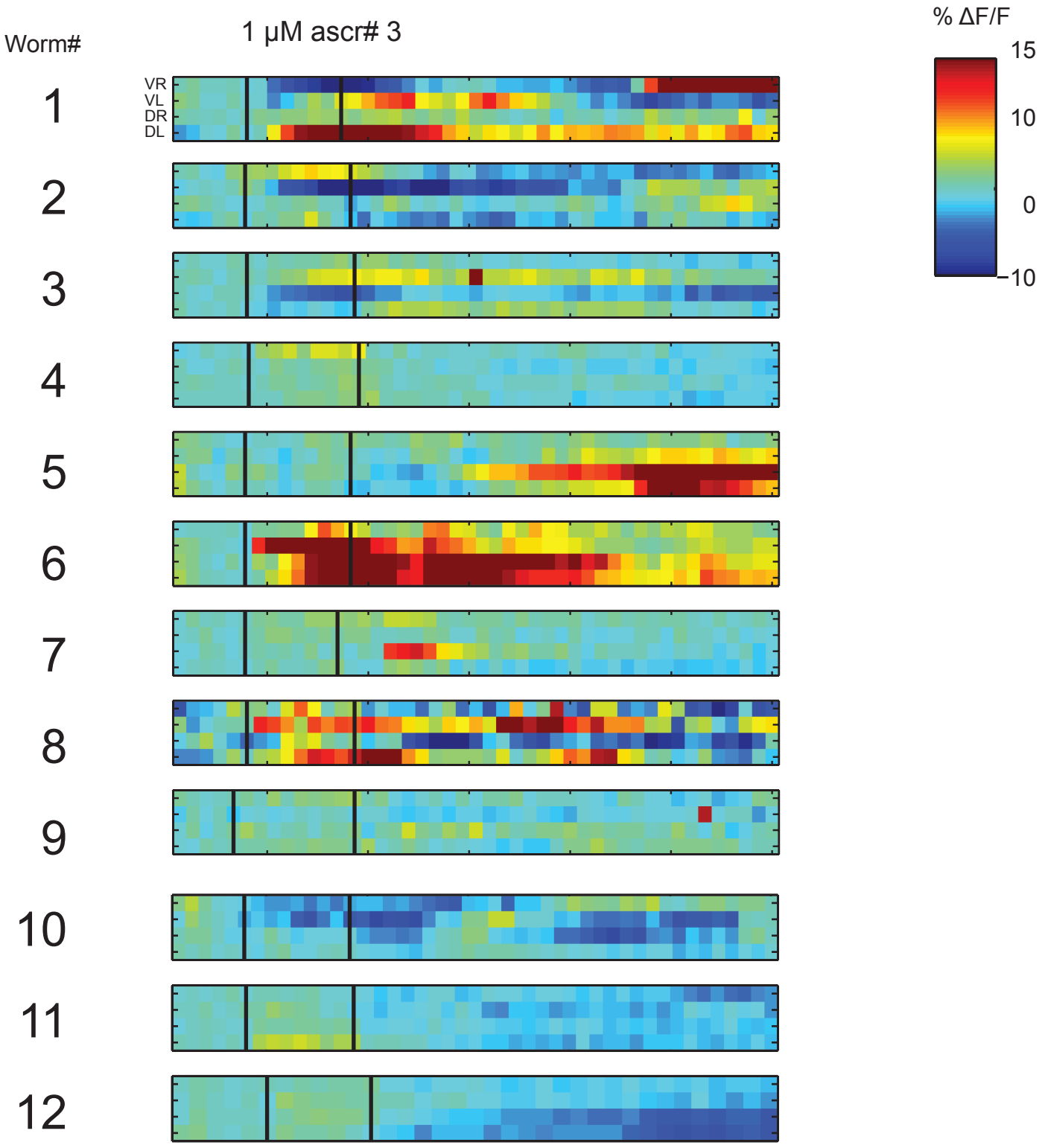

Supplementary Figure S12

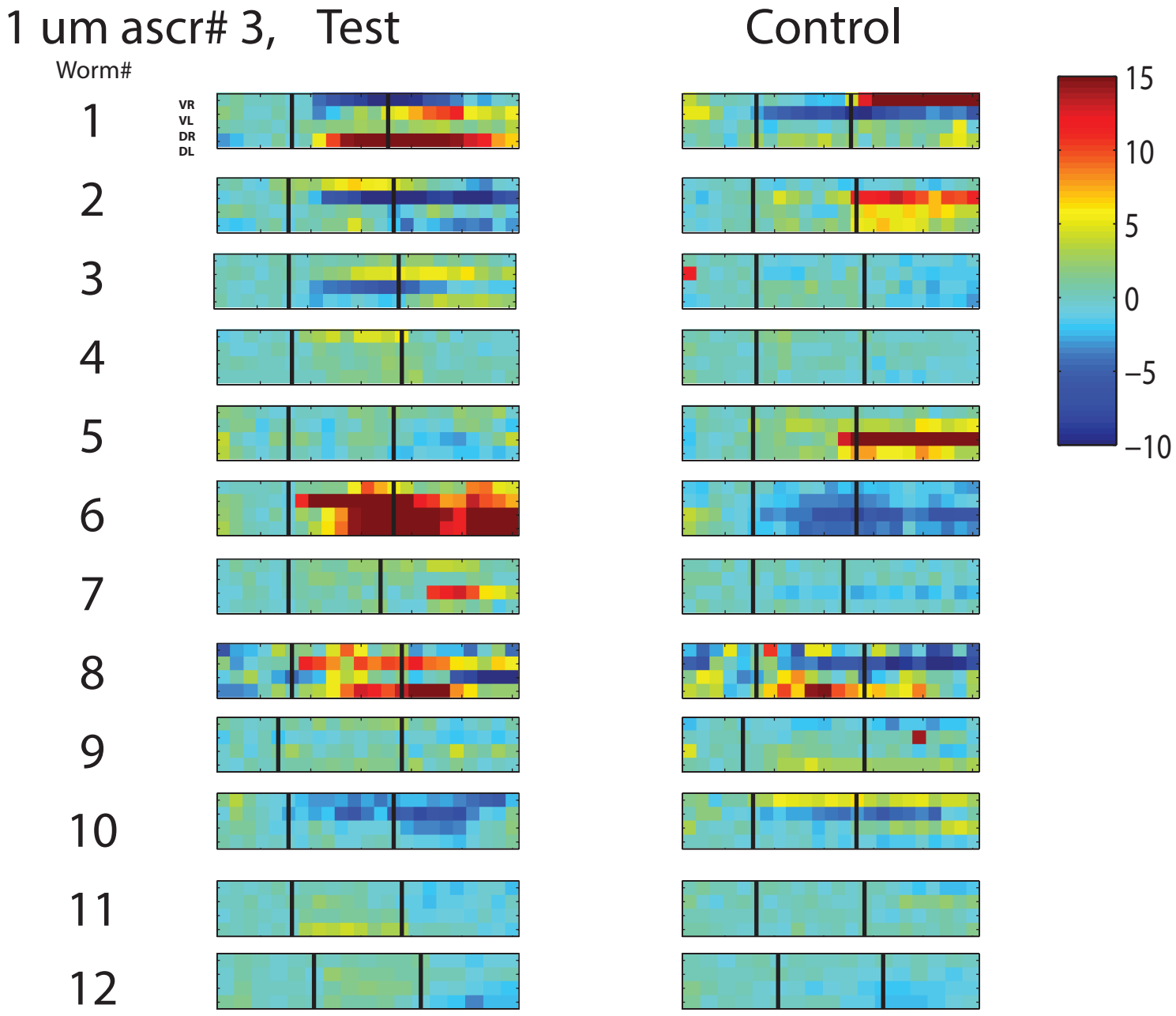

Supplementary Figure S13

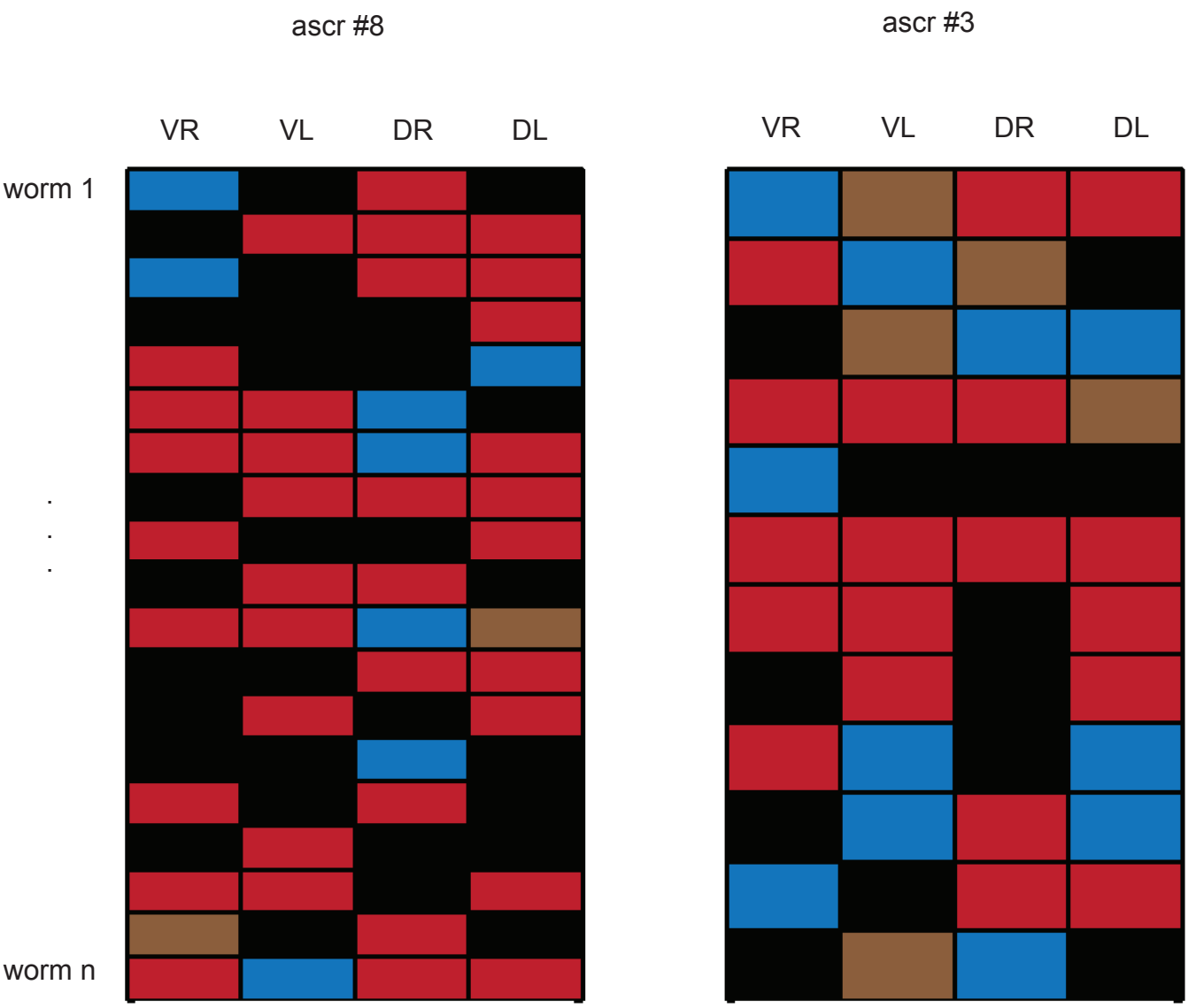

Supplementary Figure S14

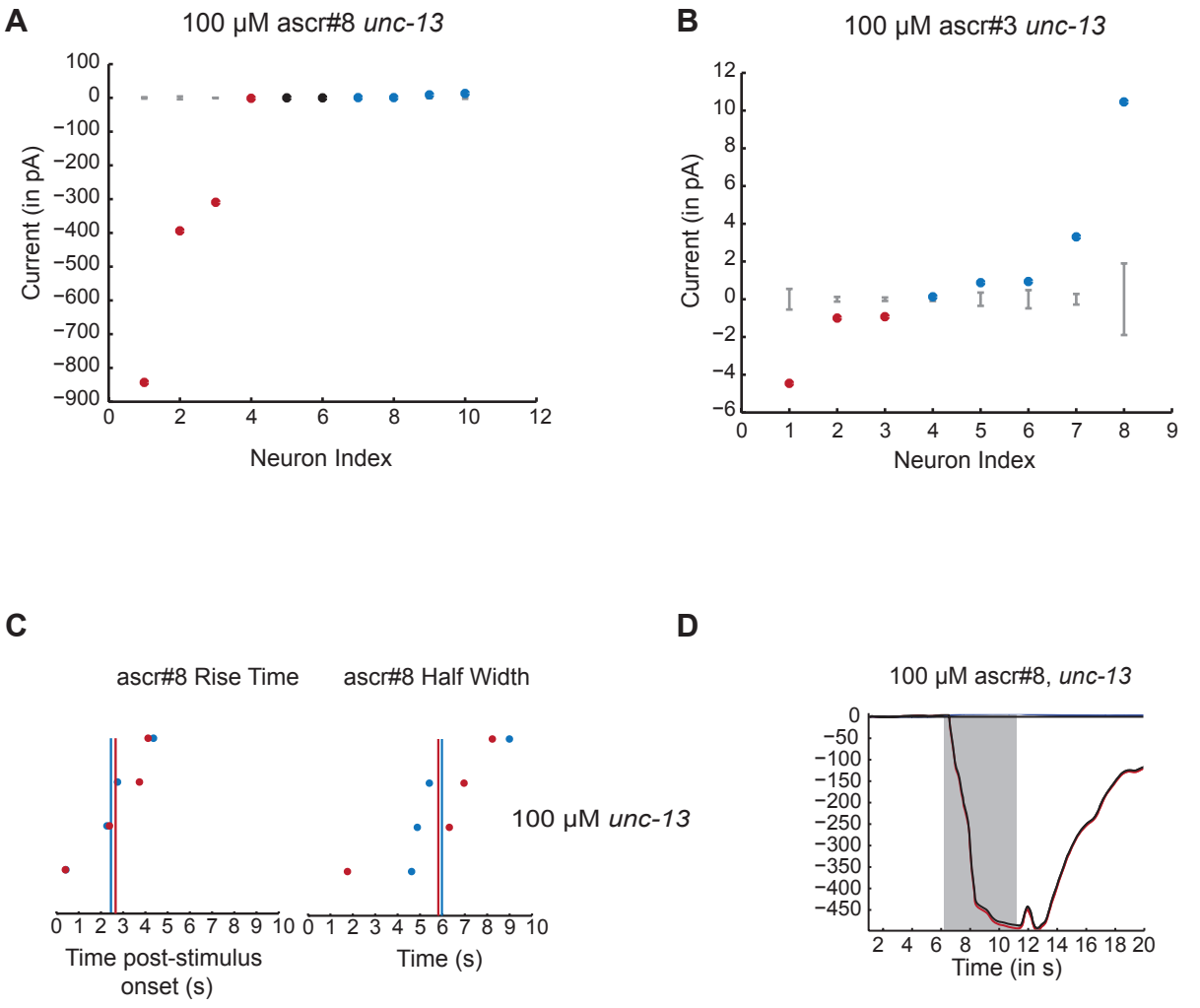

Supplementary Figure S15

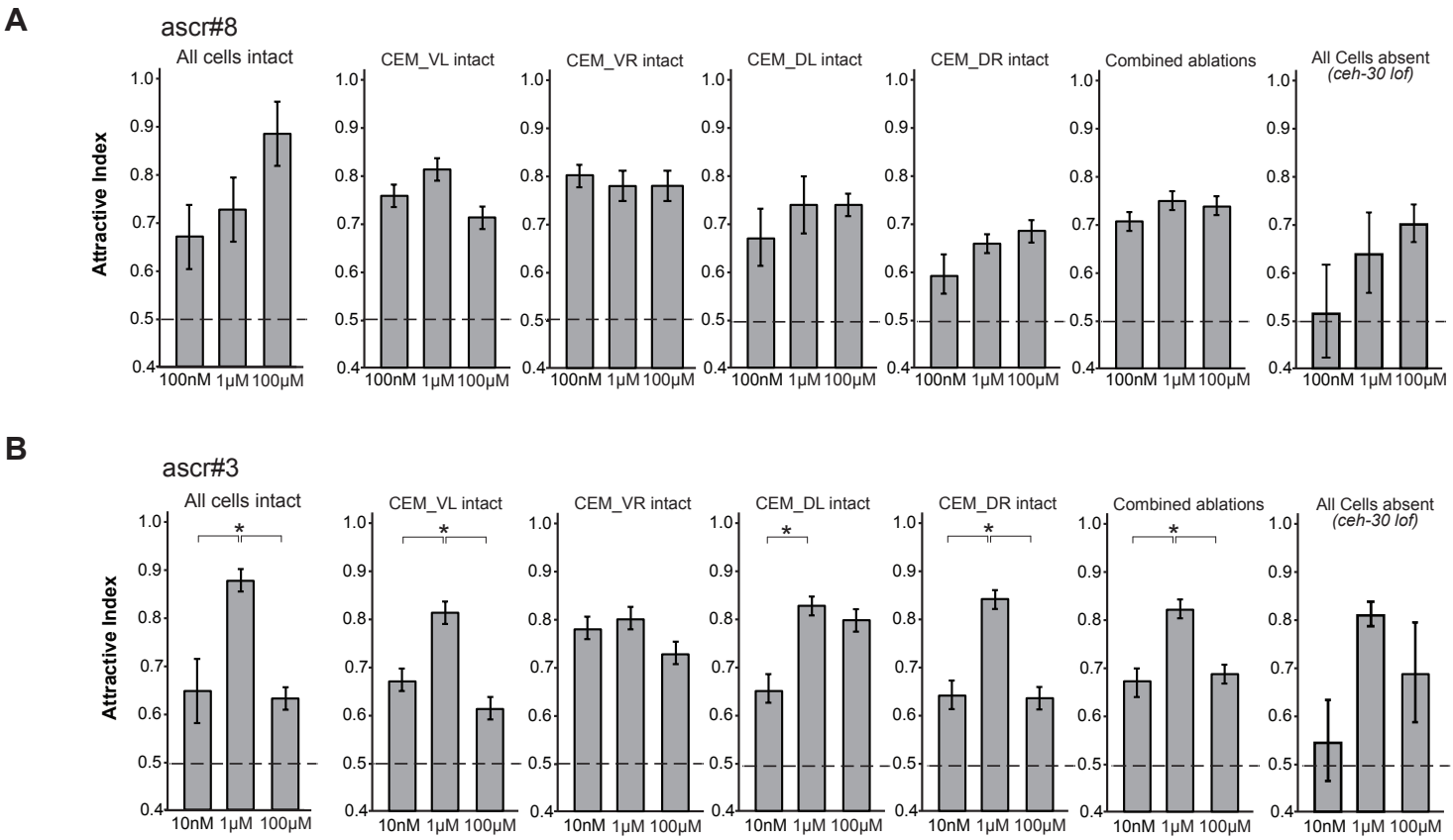

Supplementary Figure S16

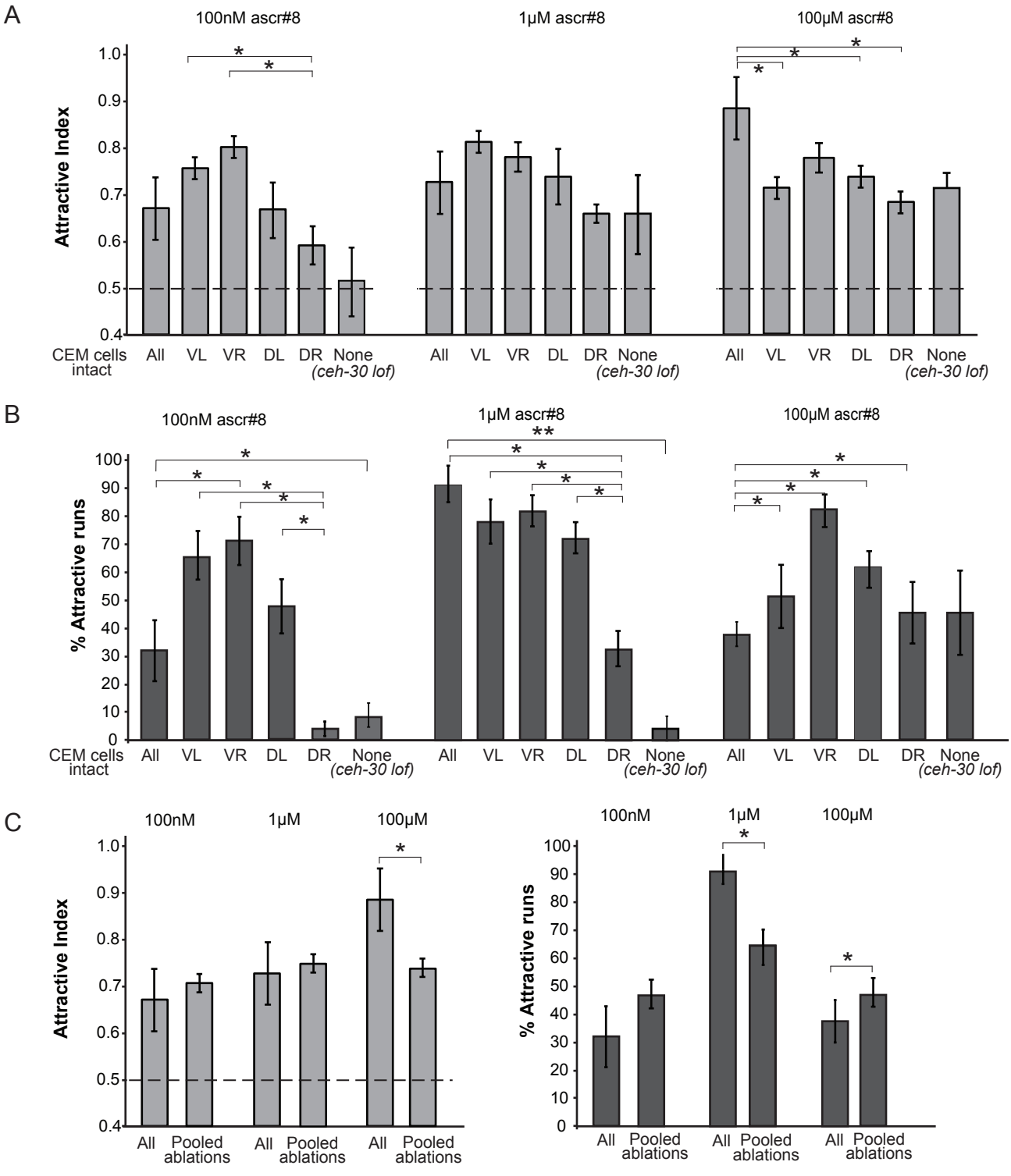

Supplementary Figure S17

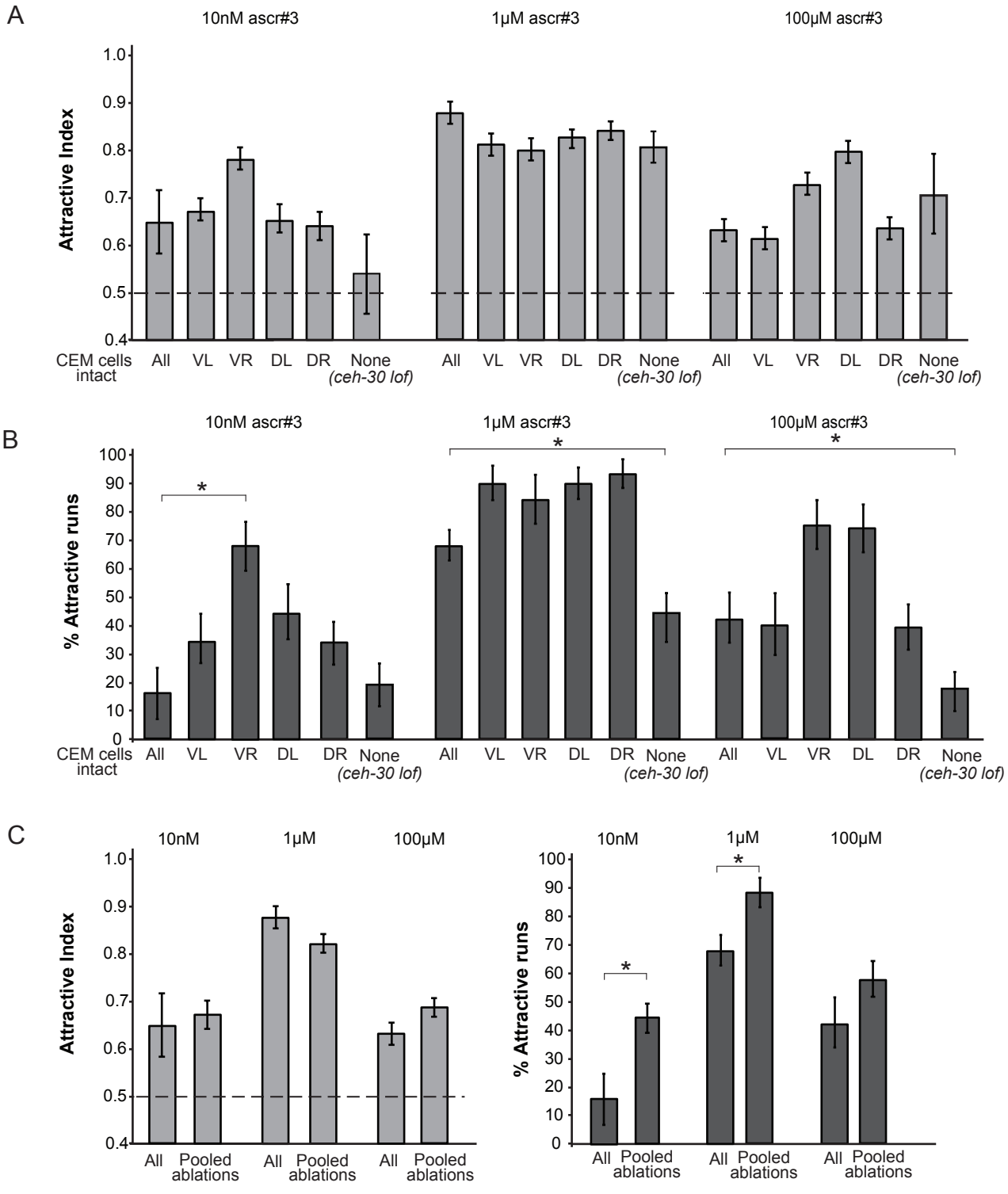

Supplementary Figure S18

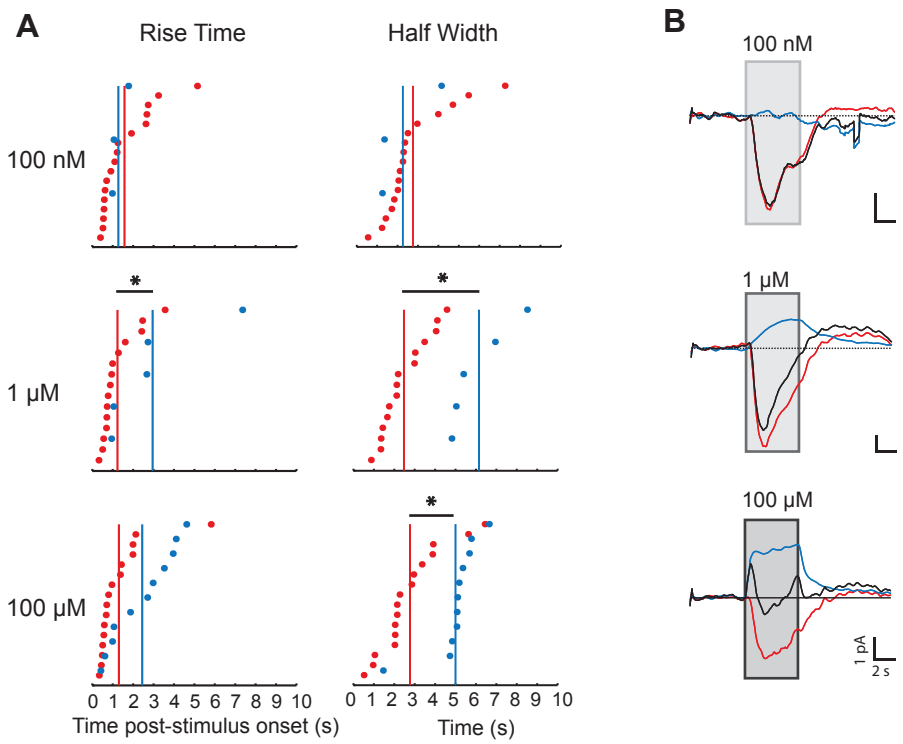

Supplementary Figure S19

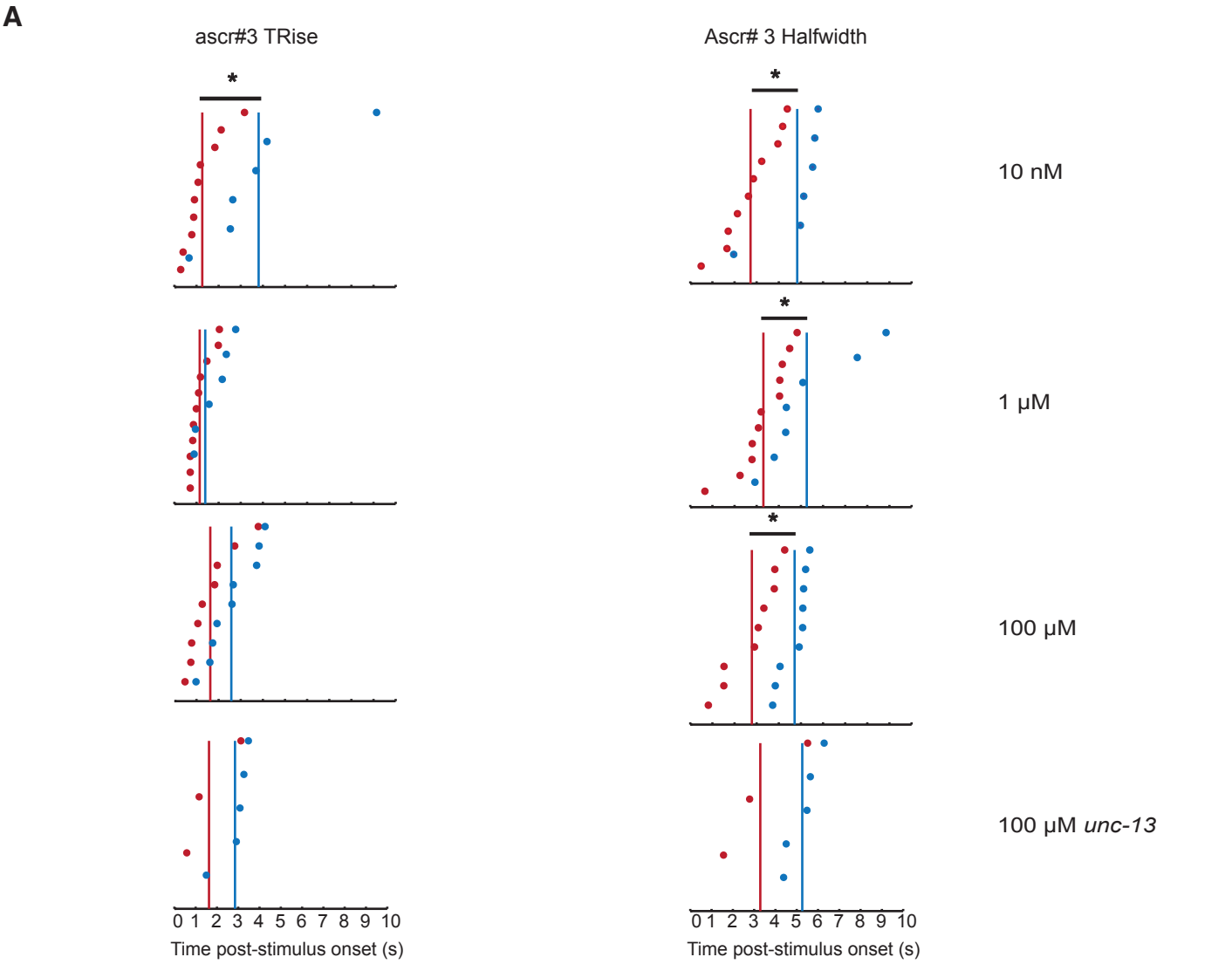

Supplementary Figure S20

Supplementary Figure Legends

Figure S1: Evoked current responses to ascarosides A) Mean evoked current response to ascr#8 over stimulus pulse at each concentration. Red, Depolarizing cells, Black, No response Cells, Blue, Hyperpolarizing cells, gray, average of all cells. **B)** Histogram of evoked responses at each concentration. Black vertical line shows mean response (corresponding to gray trace in A). **C)** Mean evoked current response to ascr#3 over stimulus pulse at each concentration. **D)** Histogram of evoked responses at each concentration of ascr#3.

Figure S2: Example traces for each mode of response to ascr# 8. Example trials from single neurons from wild-type worms exhibiting different modes in response to 100 nM, 1 µM, 100 µM ascr#8 (top 3 rows) and responses to 100 µM ascr#8 in *unc-13* worms (bottom row). Each panel represents a single recording from a different worm.

Figure S3: Fractions of neuronal population exhibiting different modes of response to ascr#8. A) Breakdown of total number of recordings in response to ascr#8 by anatomical identity of the neuron. **B)** Breakdown of cells in each location by mode of response, top row. Distribution of number of cells at each concentration, segregated by response mode, rows 2-4, and for unc-13 animals, row 5. Red, depolarizing, black, no response, blue, hyperpolarizing, brown, complex (both de- and hyperpolarizing). D, Dorsal, V, Ventral, L, Left, R, Right, X, Unknown.

Figure S4: Example traces for each mode of response to ascr#3. Example trials from single neurons from wild type worms exhibiting different modes in response to 10

nM, 1 µM, 100 µM ascr#3 (top 3 rows) and responses to 100 µM ascr#3 in *unc-13* worms (bottom row).

Figure S5: Fractions of neuronal population exhibiting different modes of response to ascr#3. A) Breakdown of total number of recordings in response to ascr#8 by anatomical identity of the neuron. **B)** Breakdown of cells in each location by mode of response, top row. Distribution of number of cells at each concentration, segregated by response mode, rows 2-4, and for *unc-13* animals, row 5. Red, depolarizing, black, no response, blue, hyperpolarizing, brown, complex (both de- and hyperpolarizing). D, Dorsal, V, Ventral, L, Left, R, Right, X, Unknown.

Figure S6: **Average responses of 'complex' neurons** in response to A) ascr#8 and B) ascr#3.

Figure S7: Example traces for complex neurons in response to both ascr#8 (A) and ascr#3 (B). Each row represents a single neuron's response to a specific concentration. From left towards right: three successive trials from the same neurons, with overlaid and average response (rightmost panel).

Figure S8: Example current clamp recording showing voltage responses to **A)** ascr#8 and **B)** ascr#3. Red, depolarizing responses, blue, hyperpolarizing responses, black, non-responsive cells, cyan, hyperpolarizing responses in *unc-13* mutants, orange, depolarizing responses in *unc-13* mutants.

Figure S9: Successively recorded neurons for individual worms show heterogeneous response modes.

Figure S10: Heat maps of GCaMP fluorescence changes evoked by 1 µM ascr#8. Each block shows Ca responses of an individual worm with each row representing the response of an individual CEM neuron in that worm, averaged over all its analyzed features (dendrite tip, dendrite, soma, axon) and over ten trials, each trial 30 seconds long. Solid vertical black lines mark stimulus onset and offset. N = 18 worms.

Figure S11: Control analyses of GCaMP fluorescence analyses changes evoked by 1 µM ascr#8. The left panel (Test), shows the first 15 seconds of each trial, comprising of 5 seconds baseline, 5 seconds stimulus, and 5 seconds post-stimulus time, analysed as in Figure S10. The Right panel (Control), shows the same analyses performed on the last 15 seconds of each trial, which is all post-stimulus, by assuming a similar structure (pre, stim, and post). Solid vertical black lines mark stimulus onset and offset, N = 18 worms.

Figure S12: Heat maps of GCaMP fluorescence changes evoked by 1 µM ascr#3. Each block shows Ca responses of an individual worm, with each row representing the response of an individual CEM neuron in that worm, averaged over all its analyzed features (dendrite tip, dendrite, soma, axon) and over ten trials, each trial 30 seconds long. Solid vertical black lines mark stimulus onset and offset. N = 12 worms.

Figure S13: Control analyses of GCaMP fluorescence analyses changes evoked by 1 µM ascr#3. The left panel (Test), shows the first 15 seconds of each trial, comprising of 5 seconds baseline, 5 seconds stimulus, and 5 seconds post-stimulus

time, analysed as in Figure S12. The Right panel (Control), shows the same analyses performed on the last 15 seconds of each trial, which is all post-stimulus, by assuming a similar structure (pre, stim, and post). Solid vertical black lines mark stimulus onset and offset, N = 12 worms.

Figure S14: CEM response mode distribution across worms for ascr#8 and ascr#3. Each square represents the assigned response mode for a given CEM, each row represents a single worm, in the same order as the heatmaps in the previous figures.

Figure S15: A) Mean evoked responses of *unc-13* worms sorted by magnitude to **A)** ascr#8,100 μM and **B)** ascr#3 100 μM. A given neuron's response was classified as depolarizing (red), hyperpolarizing (blue) or not responsive (black), based on whether the average neural response over the duration of the stimulus exceeded 2*SD of the baseline (computed over 4 seconds before stimulus, shown in gray) for that neuron. **C)** Rise time and half width of response of *unc-13* worms to ascr#8. **D)** Composite response of *unc-13* worms to ascr#8. **E)** Top: Synaptic currents evoked by 100 μM ascr#8 (computed as the difference between *wt* and *unc-13* responses) in depolarized and hyperpolarized cells are opposite in sign. Bottom, 100 μM ascr#3-evoked synaptic currents in depolarized cells occurs out of phase with synaptic responses in hyperpolarizing cells. The horizontal extent of the gray region in the bottom panel corresponds to that of the black box in the top panel **F)** breakdown of dataset by response mode at each concentration of ascr#8 (top) and ascr#3 (bottom). Red,

depolarizing mode, blue, hyperpolarizing mode, black, no response mode, brown, complex response mode.

Figure S16: Attraction Indices for behavioral responses to ascarosides #8 and #3. **A)** Attraction Index for ascr#8, for intact worms (left most panel), worms with only one of 4 CEMs intact (middle four panels) and the average of all ablated worms (rightmost panel). **B)** Attraction Index for ascr#3 at different concentrations, for intact and ablated worms.

Figure S17: Differences in behavioral responses between intact and ablated animals at each concentration of ascr#8. A) Attraction Index (AI) grouped by concentration. At low concentration, there was a significant difference in AI at $p < 0.05$ ($F(4, 63) = 4.57$, $p = 0.0027$). Post-hoc Tukey's HSD test showed that the AI values for DR were significantly different from VL as well as VR. At medium concentration, there was no significant difference in AI at $p<0.05$. $F(4,77) = 1.53$, $p = 0.2$. At high concentration, there was a significant difference in AI at $p<0.05$ ($F(4,56) = 3.78$, $p =0.0086$). Post-hoc Tukey's HSD test showed that intact worms were significantly different from DL, DR and VL. **B)** %Attractive runs, grouped by concentration. At low concentration, there was a significant difference in %Attractive runs at $p < 0.05$ ($F(4, 63) = 10.94$, $p = 8.44e-7$). Post-hoc Tukey's HSD test showed that the %attractive run values for intact and VR were significantly different, and DR was significantly different from DL, VR and VL. At medium concentration, there was a significant difference in %Attractive runs at $p<0.05$ ($F(4,76) = 10.1$, $p = 1.3 e-6$). Post-hoc Tukey's HSD test showed that the %attractive run values for DR was significantly different from all others.

At high concentration, there was a significant difference in % Attractive runs, $p < 0.05$ ($F(4,56) = 8.17$, $p = 2.92e\text{-}5$). Post-hoc Tukey's HSD test shows that the intact %attractive run values were significantly different from all others. **C)** Comparison of intact and pooled ablated animals for Attraction Index. At low concentration, there was no significant difference in AI for $p < 0.05$ ($F(1, 66) = 0.34$, $p = 0.55$). At medium concentration, there was no significant difference in AI at $p<0.05$ ($F(1,80) = 0.29$, $p = 0.59$). At high concentration, there was a significant difference in AI at $p<0.05$ ($F(1,59) = 11.69$, $p =0.0011$). Post-hoc Tukey's HSD test showed that intact was significantly different from pooled ablations. **D)** Comparison of intact and all ablated animals for % Attractive Runs. At low concentration, there was no significant difference in %Attractive Runs for $p < 0.05$ ($F(1, 66) = 1.33$, $p = 0.25$). At medium concentration, there was a significant difference in %Attractive Runs at $p<0.05$. $F(1,79) = 8.92$, $p = 0.0037$.Post-hoc Tukey's HSD test showed that intact was significantly different from pooled ablations. At high concentration, there was a significant difference in % Attractive Runs, $p < 0.05$ ($F(1,59) = 20.86$, $p =2.5e\text{-}5$). Post-hoc Tukey's HSD test showed that intact was significantly different from pooled ablations.

Figure S18: Differences in behavioral responses between intact and ablated animals at each concentration of ascr#3. A) Attractive Index, grouped by concentration. There was no significant difference in AI at any concentration. **B)** %Attractive runs, grouped by concentration. At low concentration, there was a significant difference in %Attractive runs at $p < 0.05$ ($F(4, 72) = 4.51$, $p = 0.0026$). Post-hoc Tukey's HSD test showed that the %Attractive run values for intact and VR were

significantly different. At medium concentration, there was a significant difference in %Attractive runs at $p<0.05$($F(4,104) = 4.3$, $p = 0.0029$). Post-hoc Tukey's HSD test showed that the %Attractive run values for intact and DR were significantly different. At high concentration, there was a significant difference in % Attractive runs at $p < 0.05$ ($F(4,78) = 3.59$, $p =0.0097$). Post-hoc Tukey's HSD test showed that none of the values were significantly different from each other. **C)** Comparison of intact and all ablated animals for Attractive Index. At low concentration there was no significant difference in AI at $p<0.05$, $F(1,75) = 0.53$, $p = 0.47$. At med conc., there was a significant difference in AI at $p<0.05$. $F(1,107) = 4.31$, $p = 0.0403$. Post-hoc Tukey's HSD test showed that the AI values for wt and pooled ablations were significantly different. At high conc., there was no significant difference in AI at $p<0.05$. $F(1,81) = 1.05$, $p =0.308$. **D)** Comparison of intact and all ablated animals for % Attractive Runs. At low concentration, there was a significant difference in %Attractive runs at $p <0.05$ ($F(1, 75) = 7.7$, $p = 0.0007$). Post-hoc Tukey's HSD test showed that the %attractive run values for intact and pooled ablations were significantly different. At medium concentration, there was a significant difference in %Attractive runs at $p<0.05$ ($F(1,107) = 16.54$, $p = 9.1e-5$). Post-hoc Tukey's HSD test showed that the %attractive run values for intact and pooled ablations were significantly different. At high concentration, there was no significant difference in % Attractive runs at $p < 0.05$ ($F(1,81) = 1.98$, $p =0.1637$).

Figure S19: A) Relative rise times (left column) and half-widths (right column) of de- and hyperpolarizing responses (in red and blue respectively) to ascr#8. **B**) The effective CEM output at different concentrations of ascr#8. Red, average depolarizing response,

blue, average hyperpolarizing response, black, sum of de- and hyperpolarizing response.

Figure S20: A) Relative rise times (left column) and half-widths (right column) of de- and hyperpolarizing responses (in red and blue respectively) to ascr#3. **B**) The effective CEM output at different concentrations of ascr#3 (left 3 panels) and at 100 µM ascr#3 for *unc-13* worms. Red, average depolarizing response, blue, average hyperpolarizing response, black, sum of de- and hyperpolarizing response.